IET Generation, Transmission & Distribution

Research Article

Decomposition-based approach to risk-averse transmission expansion planning considering wind power integration

ISSN 1751-8687
Received on 9th September 2016
Revised 21st December 2016
Accepted on 23rd December 2016
E-First on 27th September 2017
doi: 10.1049/iet-gtd.2016.1439
www.ietdl.org

Jing Qiu[1,2], Junhua Zhao[2,3] ✉, Dongxiao Wang[4], Zhao Yang Dong[5]

[1]*School of Electrical and Information Engineering, University of Sydney, Camperdown, NSW 2006, Australia*
[2]*School of Electrical and Information Engineering, Changsha University of Science and Technology, Changsha, Hunan, 410114, China*
[3]*School of Science and Engineering, the Chinese University of Hong Kong (Shenzhen), Longgang, Shenzhen, Guangdong, 518172, China*
[4]*Centre for Intelligent Electricity Networks, the University of Newcastle, Callaghan, NSW 2308, Australia*
[5]*School of Electrical Engineering and Telecommunications, the University of New South Wales, Kensington, NSW 2052, Australia*
✉ *E-mail: junhua.zhao@outlook.com*

Abstract: The increasing penetration of wind power (WP) and demand response (DR) programs into modern power systems poses more challenges on transmission expansion planning (TEP). To ensure the economical, secure and reliable operations of power systems, this study presents a risk-averse TEP framework. Instead of using the deterministic security criterion, an insecurity risk cost (RC) is proposed to provide network planners with the insight into the problem, options and future implications in decision making. Specifically, this RC can quantify the system security degree, considering the probability and the severity of contingencies. Meanwhile, the economic value of DR is modelled and incorporated into the optimal operation solutions. Moreover, to enhance the computational efficiency, an iterative solution algorithm based on the Benders decomposition is developed to solve the formulated TEP problem. The proposed approach is numerically verified on the Garver's 6-bus, IEEE 24-bus RTS, and 2383-bus polish systems. Case study results demonstrate that the proposed approach can effectively investigate the impacts of large-scale integration of WP and DR on system operations and planning. Moreover, the proposed risk-averse approach is economically efficient and more robust to stochastic variations.

1 Introduction

Transmission expansion planning (TEP) refers to determining when, where and what type of new transmission lines should be built in order to satisfy the growing energy demand [1]. The main objective of TEP in a deregulated power industry is to provide non-discriminatory and competitive market conditions to all stakeholders, while maintaining the system reliability [1, 2]. TEP is a complicated decision-making process, because there are a variety of types of uncertainties that should be taken into account. Generally speaking, the uncertainties can be classified into two main categories [2, 3]: () random uncertainties, such as load growth, availability of system components; (ii) non-random uncertainties, such as location of new generators and policy changes.

Moreover, to achieve energy sustainability and mitigate climate change, renewable energy such as wind power (WP) has proliferated greatly in the power generation portfolio over the past decades. Bulk injection of WP into power systems can cause bottlenecks in transmission lines. Meanwhile, the intermittency and uncertainty of WP can cause security issues. Variations in wind outputs can often be compensated by adjusting the outputs of the conventional power generators (i.e. regulation service providers). Following the applications of smart grids, demand response (DR) programs have attracted significant attention in terms of balancing WP and enhancing system efficiency [4]. DR programs can be categorised into price-based DR (e.g. time-of-use tariff) and incentive-based DR (IBDR) (e.g. direct load control). On the other hand, when DR reaches a critical market level, the uncertainty of consumer behaviour makes TEP more challenging [5]. Thus the influences of WP and DR on system security and adequacy should be comprehensively investigated.

In addition, to protect the power system against cascading outages or any form of instability, the security rule in many countries defines that the system can withstand the loss of any single component (i.e., $N-1$ secure) and sometimes the loss of a selected combination of two components (i.e. $N-2$ secure) [6]. In most cases, the system operators only check a set of credible contingencies, since studying all possible contingencies is practically impossible [7]. The conventional security criterion only considers a single contingency and security is a deterministic criterion. This means that all contingencies are equally treated and each should satisfy the security requirement in system operations [8]. The conventional approach can only provide a binary answer to the system security, i.e. either secure or insecure. More importantly, the deterministic approach cannot recognise the inherent probabilistic nature of system behaviours, such as customer demands and component failures [8]. Therefore, there is an interest to study the insecurity risk involved in transmission investment in the future, yielding risk-averse TEP [9].

In the literature, there are many studies addressing TEP uncertainties (e.g. load or WP variations). For instance, reference [10] has proposed a stochastic coordination of generation and transmission expansion planning model. Monte–Carlo (MC) simulations are used to capture the uncertainties of random outages of system components, as well as load forecast errors. In [11], TEP is formulated as a renovated mixed integer linear programming problem. The line investment cost (IC) and load forecast errors are considered as planning uncertainties. A robust optimisation methodology is applied to assess different levels of uncertainty and conservation. In [12], the uncertainties of remote WP and load are represented by two dependent random variables. They are considered into the two-stage stochastic optimisation model, which is then solved by the sequential approximation approach. In [13], the interactions between large-scale WP integration and TEP are analysed. The co-optimisation of energy and ancillary services is solved by the Benders decomposition technique. The authors use the MC simulations to model the various uncertainties in system operation and planning, but do not specify what types of uncertainties they have considered. In [14], the impact of high WP penetration on security and operations in the reserve market has been investigated. Moreover, in some studies, TEP only deals with the normal condition, and the worst case is modelled (i.e. peak load and no generation rescheduling), such as [15, 16]. On the other hand, there are some TEP studies addressing the security issues under $N-1$ contingencies, such as [17, 18]. Reference [17] has included the probabilistic reliability criterion into TEP. In [19], a multi-stage security constrained TEP model is proposed, and is solved by a mixed-integer linear programming approach. In [20] a TEP model is proposed to minimise the IC and the curtailed wind energy over the planning period. A probabilistic method based on clustering is used for determining the load and WP models. Unfortunately, the above-mentioned models fail to investigate the impacts of emerging DR on system economy and reliability. Furthermore, some studies contemplate the risk in TEP, such as [21, 22]. In [21], a TEP model based on risk/investment is proposed. Results are compared with those obtained by the scenario analysis method. In these studies, expected energy not supplied (EENS) or other similar reliability measures are calculated by minimising the total load curtailment repeatedly while considering generation re-dispatch (i.e. corrective control (CC) actions) under different normal and contingency scenarios. Thus the optimality and feasibility of CC actions are not well addressed, e.g. generation ramping constraints or re-dispatch costs are not considered. In [23], adaptation cost has been chosen as a flexibility measure of planning alternatives. In [24], a risk-based TEP approach is proposed to address deliberate outages. Risk characterisation is implemented through the minimax weighted regret paradigm. In addition, investigating the impact of DR on TEP is relatively a new topic, a few studies are found such as [1, 4]. Li *et al*. [4] presents a probabilistic TEP model considering large-scale wind farms integration and IBDR. The wind speed correlation between wind farms is modelled by a multi-state wind farm model. However, these references have not taken into account the upward DR (load increment). As a result, in their models, the DR's role in balancing WP fluctuations (e.g. underestimated WP outputs) is neglected.

To bridge the research gaps in the literature, in this paper a risk-averse TEP model is proposed for power systems with large-scale integration of WP and DR. Compared with the existing works in the literature, the novel contributions and salient features are fourfold: (i) A straightforward risk index is proposed to quantitatively measure the system static security. The probabilistic nature is captured, and a severity function based on generation rescheduling and load curtailment (i.e. CC actions) is developed. (ii) The economic value of DR is modelled, and its impact on system security and adequacy has been investigated. (iii) The insecurity risk cost (RC) and the DR cost (DRC) are optimally integrated into the objective function and a stochastic planning framework is developed. This framework can coordinate the optimal planning and operation solutions, and gives the network planners the ability to hedge against the risks in relation to uncertainties. (iv) Based on the Benders decomposition technique, the formulated TEP problem is decomposed into a mater problem and two salve subproblems, and they are solved iteratively until there is no violation. In case studies, the proposed approach is verified on the Garver's 6-bus, IEEE 24-bus RTS and 2383-bus Polish systems. Comparative studies are also undertaken.

The remaining paper is organised as follows: in Section 2, models of the studied uncertainties are introduced, followed by the proposed risk-averse TEP model in Section 3. The solution algorithm is explained in Section 4. Section 5 presents numerical simulations to demonstrate the effectiveness of our approach. Finally, conclusions are given in the last section.

2 Uncertainties modelling

2.1 Demand response model

This paper only focuses on the IBDR. Incentives are paid to customers who reduce or increase their energy consumption when requested, and customers participate in the market dispatch through DR bids. For instance, power demands of electric vehicle charging/discharging, and heating ventilation and air conditioning are elastic and can be considered as IBDR. The economic values of DR resources are modelled as follows.

It is assumed that the DRC y and the load adjustment $P_{\rm DR}$ (including $P_{\rm DR}^-$ and $P_{\rm DR}^+$) can be represented by a linear function given in (1) [25, 26]. Note that $P_{\rm DR}^-$ means load decrement, while $P_{\rm DR}^+$ means load increment.

$$y = \ell_2 + \ell_1 P_{\rm DR} \tag{1}$$

where y is the price at which a consumer is willing to accept in \$/MWh, ℓ_2 is the intercept (in \$/MWh), and ℓ_1 is the slope (in \$/MW^{2}h).

To avoid creating new demand peaks, the maximum demand at each demand bus is introduced below.

$$\begin{cases} P_{\rm D} - P_{\rm DR}^- \geq 0 \\ P_{\rm D} + P_{\rm DR}^+ \leq P_{\rm D}^{\rm Max} \end{cases} \tag{2}$$

$$P_{\rm DR}^- \geq 0, \quad P_{\rm DR}^+ \geq 0 \tag{3}$$

where $P_{\rm D}^{\rm Max}$ denotes the upper bound of demand; $P_{\rm D}$ denotes power demand.

The bid price $C_{\rm DR}$ of load adjustment (load increment and decrement) of customers can be modelled by a quadratic form in (4) [27, 28]. Equation (5) states that negative $P_{\rm DR}$ means load increment; while positive $P_{\rm DR}$ means load decrement. Equation (6) states the maximum DR ratio ρ. In addition to the quadratic form of DRC as reported in [27], other mathematical forms are also found, such as linear, exponential and logarithmic functions [29]. The bid uncertainty of DR can be modelled by the Gaussian distribution [4].

$$C_{\rm DR} = \frac{1}{2}\ell_1 P_{\rm DR}^2 + \ell_2 P_{\rm DR} \tag{4}$$

$$P_{\rm DR} = \begin{cases} P_{\rm DR}^-, & \text{if } P_{\rm DR} \geq 0 \\ -|P_{\rm DR}^+|, & \text{else} \end{cases} \tag{5}$$

$$\frac{|P_{\rm DR}|}{P_{\rm D}} \leq \rho \tag{6}$$

2.2 Other uncertainties

In this paper, DR bids, load forecast errors, WP outputs and component availability are considered as uncertainties. The uncertainties are represented by probability density functions (PDFs). Wind speed is approximately modelled by the Weibull distribution [30]. For simplicity, the spatial and temporal correlation between wind farms is not considered. The WP output is calculated using the power-speed curve [30]. It is worth mentioning that in addition to the Weibull distribution, the Kaimal turbulence model can also be used to model the wind speed. Reference [31] has proposed a high-order sliding-mode control strategy to regulate the WP outputs. The proposed strategy in [31] is robust to the parametric uncertainties of the wind turbine. Furthermore, load forecast errors and IBDR bid are modelled by the Gaussian distribution [4]. Forced outage rates (FORs) are modelled by the Binomial distribution [8]. The mathematical formulations of these PDFs are common in the literature and they are not given in detail. For example, a scenario can be: 'for $t = 1$, WP output is 100 MW, load level is 2500 MW, DR bid price is \$70/MWh, and all components are available.' Moreover, the $2m+1$ estimate scheme is employed to perform probabilistic optimal power flow (POPF), which simulates the market dispatch. Its technical details can be found in [32], and is hence not repeated here.

3 Risk-averse TEP model

3.1 Objective

To better capture the effect of DR, the proposed TEP model is static and chronological (i.e. TEP for a single stage and one year is modelled by 8760 h) [18]. The objective function comprises four parts: line IC, DRC, power generation cost (GC), and insecurity RC, as seen in (7). Mathematically, risk value is calculated as the summation of the products of the probability and the severity of a threat event [33]. Thus the insecurity RC is calculated based on the probabilities and the severities of contingencies.

$$\sum_{(i,j) \in \Omega_N} C_{Lij}\eta_{ij} + \sum_{t=1}^{8760}\sum_{i=1}^{\Omega_D} C_{\mathrm{DR}0it} + \sum_{t=1}^{8760}\sum_{i=1}^{\Omega_G} C_{Oit} + \sum_{t=1}^{8760} R_t \tag{7}$$

where subscript 0 denote the normal condition, subscript t denotes time; subscripts i or j denote bus; Ω_N, Ω_G, Ω_D denote sets of all buses, generators, demand buses, respectively.

The detailed calculations of (7) are given below.

$$C_{Lij} = \mathrm{LCF} \cdot L_{ij} \tag{8}$$

$$C_{\mathrm{DR}0it} = \frac{1}{2}\ell_1 P_{\mathrm{DR}0it}^2 + \ell_2 P_{\mathrm{DR}0it}, \quad i \in \Omega_D \tag{9}$$

$$C_{Oit} = a_{1i}P_{\mathrm{G}0it}^2 + a_{2i}P_{\mathrm{G}0it} + a_{3i}, \quad \forall i \in \Omega_G \tag{10}$$

$$R_t = \sum_{k=0}^{K} \mathrm{Pr}_{kt} \cdot \mathrm{CC}_{kt} \tag{11}$$

$$\mathrm{CC}_{kt} = \begin{cases} \sum_{i \in \Omega_G} \alpha_{Gi} \cdot (P_{\mathrm{G}kit} - P_{\mathrm{G}0it})^2, & \text{if } \sum_{i \in \Omega_D} P_{\mathrm{D}t0i} = \sum_{i \in \Omega_D} P_{\mathrm{D}kti} \\ \sum_{i \in \Omega_D} C_{\mathrm{DR}kit} + \mathrm{VCR} \cdot \sum_{i \in \Omega_D} P_{kit}^{\mathrm{Curt}}, & \text{else} \end{cases} \tag{12}$$

$$\sum_{i \in \Omega_G} \alpha_{Gi} \cdot (P_{\mathrm{G}kit} - P_{\mathrm{G}0it})^2 = \sum_{i \in \Omega_G} \alpha_{Gi}P_{\mathrm{G}kit}^2 - 2\alpha_{Gi}P_{\mathrm{G}0it}P_{\mathrm{G}kit} + \alpha_{Gi}P_{\mathrm{G}0it}^2 \tag{13}$$

where LCF denotes line cost factor (a constant); L_{ij} is the length between $i-j$; η_{ij} denotes the number of lines should be built between $i-j$; a_{1i}, a_{2i}, a_{3i} are generator cost coefficients; $P_{\mathrm{G}0it}$, $P_{\mathrm{G}kit}$ denote thermal power outputs in normal and contingency conditions, and they are subject to ramping constraints; Pr_{kt} denotes the probability of contingency k at time t; K denotes the total number of credible contingencies considered; CC_{kt} is the CC cost function; $P_{\mathrm{D}kit}^{\mathrm{Curt}}$ denotes the involuntary load curtailment in contingency k at time t bus i; VCR denotes value of customer reliability. Note that when performing the deterministic security evaluation, Pr_{tk} is set to be 1 as a constant. In practice, this probability is subject to the impacts of line length or voltage level, weather, aging and geographic locations [15]. Equation (12) is the severity function of contingencies, which is calculated by the cost of CC actions such as generation rescheduling and load curtailment. Note that the severity function in (12) is not unique, the approach developed in this paper can easily be adapted if other severity functions are adopted. The upper part in (12) means generation rescheduling is used alone, while the lower part means load curtailment is used (including DR and involuntary load curtailment). Note that in (12) the load curtailments under normal and contingency conditions have been all considered (i.e. $k = 0, 1, 2, \ldots, K$). As seen in (13), generation rescheduling cost is in the same form as the GC function (10) since α_{Gi} and $P_{\mathrm{G}0it}$ are scalars, with a_{1i}, a_{2i}, a_{3i} being replaced by α_{Gi}, $-2\alpha_{Gi}P_{\mathrm{G}t0i}$, $\alpha_{Gi}P_{\mathrm{G}t0i}^2$. Other formulations of CC cost can also be used depending on the practical needs. In this paper, CC is just a term used to describe generation re-dispatch and load curtailment, according to [34]. The optimality and feasibility of CC actions are considered, in order to quantify the severity of contingencies. In the meantime, EENS (i.e. the reliability measure) is calculated based on the mean value of load curtailments under both normal and contingency conditions. To sum up, the control and the operation of the system are both implemented at the long-term TEP level. They are used to evaluate the security and adequacy of the network in the long-term.

3.2 Constraints

The constraints are below, including nodal balances, generator capacity constraints, branch flow constraints, ramping constraints, DR and load curtailment constraints, and constraints of decision variables.

(i) Power balance constraint

$$\sum_{i,j \in \Omega_N} S_{0ijt} + \sum_{i \in \Omega_G} (P_{\mathrm{G}0it} + P_{\mathrm{GW}0it}) = \sum_{i \in \Omega_D} \left(P_{\mathrm{D}0it} - P_{0it}^{\mathrm{Curt}} - P_{\mathrm{DR}0it}\right) \tag{14}$$

$$\sum_{i,j \in \Omega_N} S_{kijt} + \sum_{i \in \Omega_G} (P_{\mathrm{G}kit} + P_{\mathrm{GW}kit}) = \sum_{i \in \Omega_D} \left(P_{\mathrm{D}kit} - P_{kit}^{\mathrm{Curt}} - P_{\mathrm{DR}kit}\right) \tag{15}$$

where subscripts t, k, i or j denote time, kth contingency, and bus, respectively; P_{GW} denotes WP output; S denotes power flow; P_{D} denotes power demand. Equations (14) and (15) state node balance in normal (pre-contingency) and post-contingency conditions, respectively. Note that in order to avoid repeated information, subscripts 0 or k are removed in the constraints below.

(ii) Generator capacity constraint

$$0 \le P_{\mathrm{G}it} \le \overline{P}_{\mathrm{G}i} \tag{16}$$

$$0 \le P_{\mathrm{GW}it} \le \overline{P}_{\mathrm{GW}i} \tag{17}$$

(iii) Branch flow constraint

$$S_{ijt} - \gamma_{ij}\left(\eta_{ij}^0 + \eta_{ij}\right)\left(\theta_{it} - \theta_{jt}\right) = 0 \tag{18}$$

$$\left|S_{ijt}\right| \le \left(\eta_{ij}^0 + \eta_{ij}\right)\overline{S}_{ij} \tag{19}$$

(iv) Ramping constraint

$$\begin{cases} P_{\mathrm{G}i,t} - P_{\mathrm{G}i,t-1} \le \mathrm{RU}_i \\ P_{\mathrm{G}i,t-1} - P_{\mathrm{G}i,t} \le \mathrm{RD}_i \end{cases}, \quad i \in \Omega_G \tag{20}$$

(v) DR or load curtailment constraint

$$\begin{cases} P_{\mathrm{D}it} - P_{\mathrm{DR}it}^{-} \ge 0 \\ P_{\mathrm{D}it} + P_{\mathrm{DR}it}^{+} \le P_{\mathrm{D}it}^{\mathrm{Max}} \end{cases}, \quad i \in \Omega_D \tag{21}$$

$$P_{\mathrm{DR}it}^{-} \ge 0, \quad P_{\mathrm{DR}it}^{+} \ge 0 \tag{22}$$

$$\frac{\left|P_{\mathrm{DR}it}\right|}{P_{\mathrm{D}it}} \le \rho_{it}, \quad i \in \Omega_D \tag{23}$$

$$0 \le P_{\mathrm{DR}it} \le P_{\mathrm{D}it}, \quad i \in \Omega_D \tag{24}$$

$$0 \le P_{it}^{\mathrm{Curt}} \le P_{\mathrm{D}it}, \quad i \in \Omega_D \tag{25}$$

(vi) Decision variable constraint

$$0 \le \eta_{ij} \le \overline{\eta}_{ij}, \quad \eta_{ij} \text{ is integer}, \quad (i,j) \in \Omega_N \tag{26}$$

where $\overline{(\bullet)}$ denotes the upper bound; η^0, γ are the number of existing lines and susceptance; θ denotes phase angle; RU, RD

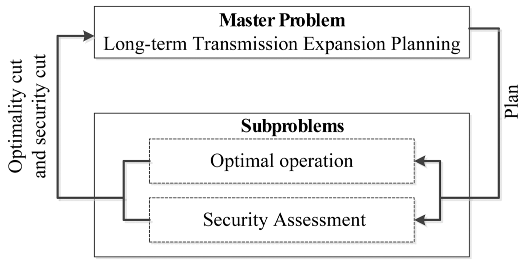

Fig. 1 *Proposed decomposition strategy for TEP*

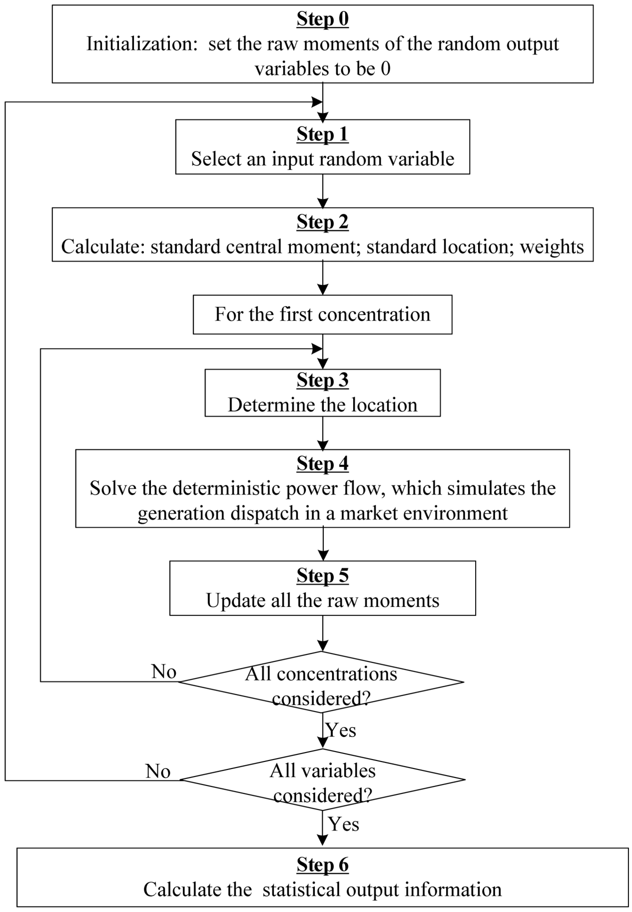

Fig. 2 *Flow chart of the applied POPF*

denote the up and down ramping limits of thermal power generators.

(vii) Reliability constraint

$$\sum_{k=0}^{K}\sum_{t=1}^{8760}\sum_{i\in\Omega_D} P_{kit}^{\mathrm{Curt}} = \mathrm{EENS} \le \overline{\mathrm{EENS}} \tag{27}$$

where EENS denotes EENS, which is a reliability measure.

4 Solution algorithm

4.1 Decomposition strategy

The original mixed integer non-linear programming problem in Section 3 is decomposed into a master problem and two slave subproblems, and they are solved iteratively until no violation exists. It is worth mentioning that for non-convex problems, the decomposition methods cannot always guarantee a global optimal solution. Nevertheless, a feasible solution that is close to the optimal one can be expected [35–37]. As seen in Fig. 1, the master problem is an integer programming problem that identifies the optimal expansion plans. The slave subproblems identify the optimal operation and assess the system security with the planning schemes given by the previous master problem. If any violation exists, Benders cuts (or similar optimality and security cuts) are generated and added to the master problem for solving the next iteration. These cuts are mainly imposed by line flow limits, since when overflow occurs, load at some buses may be curtailed, including voluntary and involuntary load curtailments. The flow chart of the applied point estimation algorithm is illustrated in Fig. 2

4.2 Optimal operation subproblem 1

The solution of the optimal operation subproblem measures the total operation cost (power generation and DRCs) for the plan identified by the master problem under the normal condition.

$$\min\{O_1\} = \min\left\{\sum_{t=1}^{8760}\sum_{i=1}^{\Omega_G} C_{Oit} + \sum_{t=1}^{8760}\sum_{i=1}^{\Omega_D} C_{\mathrm{DR}0it}\right\} \tag{28}$$

The calculations of $C_{\mathrm{DR}0it}$ and C_{Oit} are given in (9) and (10).

The constraints are as follows.

$$\sum_{i,j\in\Omega_N} S_{0ijt} + \sum_{i\in\Omega_G}(P_{\mathrm{G}0it} + P_{\mathrm{GW}0it}) = \sum_{i\in\Omega_D}\left(P_{\mathrm{D}0it} - P_{0it}^{\mathrm{Curt}} - P_{\mathrm{DR}0it}\right) \tag{29}$$

$$\left|S_{0ijt} - \gamma_{ij}(\eta_{ij}^0 + \eta_{ij}^n)(\theta_{0it} - \theta_{0jt})\right| \le (1-\chi_{ij})\cdot\mathrm{DF} \tag{30}$$

$$\left|S_{0ijt}\right| \le (\eta_{ij}^0 + \eta_{ij}^n)\overline{S}_{ij} \tag{31}$$

where η_{ij}^n is the solution obtained at the nth Benders iteration; DF is a disjunctive factor and χ_{ij} is a binary variable. If χ_{ij} is 1, meaning a power line exists or is to be reinforced, then the DC power flow equation is in effect; otherwise, if a power line is in contingency or not planned, χ_{ij} is 0, then the disjunctive factor ensures the constraint is not binding.

In addition, constraints (16)–(17), (20)–(27) must be met, with a superscript 0 denoting the normal condition (pre-contingency).

4.3 Security assessment subproblem 2

The security assessment subproblem is to minimise the total insecurity risk under all credible contingencies considered.

$$\min\{O_2\} = \min\left\{\sum_{t=1}^{8760} R_t\right\} \tag{32}$$

The calculations of R_t is given in (11) and (12)

The constraints are as follows.

$$\sum_{i,j\in\Omega_N} S_{kijt} + \sum_{i\in\Omega_G}(P_{\mathrm{G}kit} + P_{\mathrm{GW}kit}) = \sum_{i\in\Omega_D}\left(P_{\mathrm{D}kit} - P_{kit}^{\mathrm{Curt}} - P_{\mathrm{DR}kit}\right) \tag{33}$$

$$\left|S_{kijt} - \gamma_{ij}(\eta_{ij}^0 + \eta_{ij}^n)(\theta_{kit} - \theta_{kjt})\right| \le (1-\chi_{ij})\cdot\mathrm{DF} \tag{34}$$

$$\left|S_{kijt}\right| \le (\eta_{ij}^0 + \eta_{ij}^n)\overline{S}_{ij} \tag{35}$$

In addition, constraints (16)–(17), (20)–(27) must be met, with a superscript k denoting the contingency.

4.4 Master problem

The master problem takes into account the optimality and security cuts formulated at the all previous iterations and identifies the new lines to build at iteration. This problem is to minimise the IC of building new lines subject to constraints provided by the subproblems. The master problem is as follows.

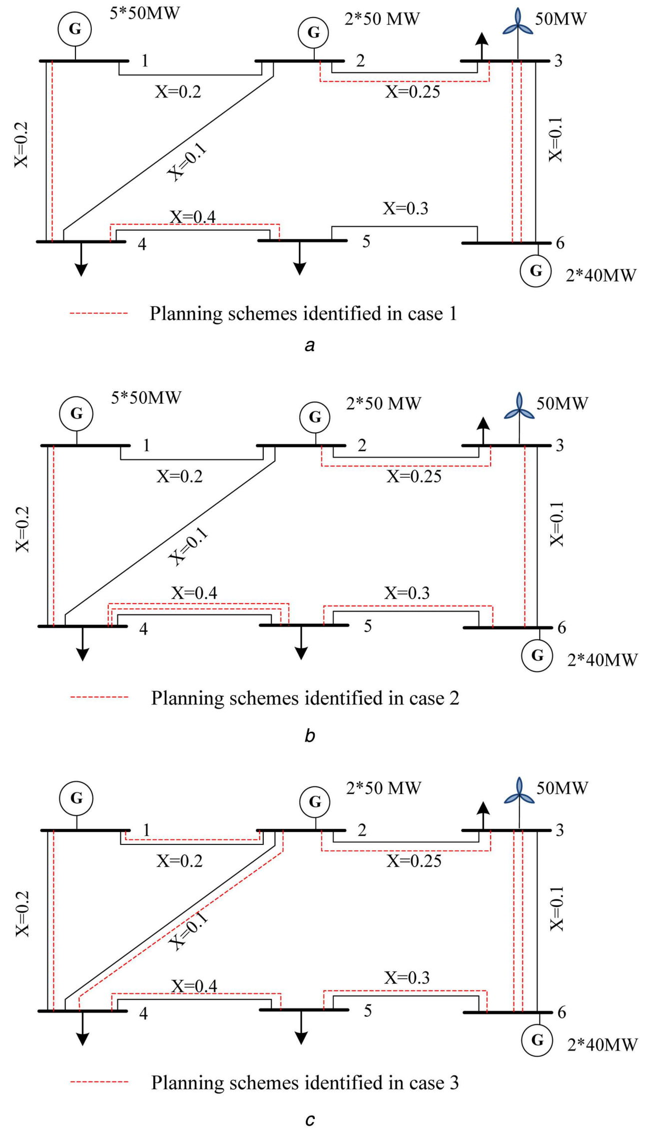

Fig. 3 *One-line diagram of 6-bus system and identified planning schemes for cases 1–3*
(a) Planning schemes identified in case 1, ***(b)*** Planning schemes identified in case 2, ***(c)*** Planning schemes identified in case 3

$$\min\left\{\sum_{(i,j)\in\Omega_N} C_{ij}\eta_{ij} + \mathrm{SV}_1 + \mathrm{SV}_2\right\} \tag{36}$$

subject to

$$O_1^n - \sum_{(i,j)\in\Omega_N} \delta_{ijt}^n(\eta_{ij} - \eta_{ij}^n) \le \mathrm{SV}_1, \quad n = 1, 2, \ldots, N \tag{37}$$

$$O_2^n - \sum_{(i,j)\in\Omega_N} \delta_{ijt}^n(\eta_{ij} - \eta_{ij}^n) \le \mathrm{SV}_2, \quad n = 1, 2, \ldots, N \tag{38}$$

$$\mathrm{SV}_1 \ge 0; \quad \mathrm{SV}_1 \ge 0 \tag{39}$$

where O_1^n, O_2^n denote the solutions of subproblems 1 and 2 of the previous iteration n; δ_{ijt}^n is the sensitivity of the optimal values O_1^n and O_2^n with respect to the decision variable η_{ij}^n; SV_1, SV_2 are the slack variables. Equations (37) and (38) are optimality and security cuts, respectively.

The calculation of sensitivity factors is given by

$$\delta_{ijt} = \pi_{ijt}\overline{S}_{ij} \tag{40}$$

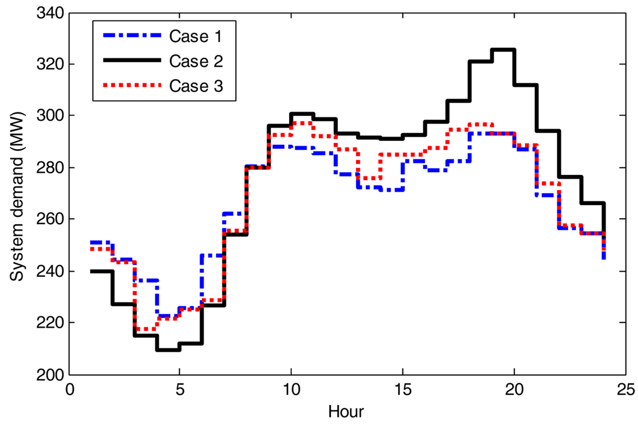

Fig. 4 *System daily average load profiles for cases 1–3*

where π_{ijt} denotes the Lagrange multipliers of (14) and (15) associated to constraints (29) and (33) in optimal operation and security assessment subproblems.

For the DC power flow model, the sensitivity factor is given:

$$\delta_{ijt} = \sum_{(i,j)\in\Omega_N} (\pi_{it} - \pi_{jt})(\theta_{it} - \theta_{jt})\gamma_{ij} \tag{41}$$

The probabilistic formulations of the cuts added to the master problem are as follows:

$$E(O_1^n) - \sum_{(i,j)\in\Omega_N} E(\delta_{ijt}^n)(\eta_{ij} - \eta_{ij}^n) \le \mathrm{SV}_1, \quad n = 1, 2, \ldots, N \tag{42}$$

$$E(O_2^n) - \sum_{(i,j)\in\Omega_N} E(\delta_{ijt}^n)(\eta_{ij} - \eta_{ij}^n) \le \mathrm{SV}_2, \quad n = 1, 2, \ldots, N \tag{43}$$

5 Case studies

5.1 Experiment setting

The proposed risk-averse TEP approach is tested on the Garver's 6-bus, IEEE 24-bus RTS and 2383-bus Polish systems. Network data can be found in [38–40], respectively. FORs of power generating units and transmission lines for the Polish system are assumed to be 0.02 and 0.01, respectively. We assume that the network needs to be expanded for the next five years and the annual load growth rate is 5%. The capacity of new power lines is 120 MW, and up to three lines are allowed on each corridor. The line IC is assumed to be 55 M$/100 km. DR resources are located at all load buses and the mean of bid price can be found in [4]. The maximum ratio of DR is 10%. The cut-in, cut-out and rated speeds of wind turbines are 4.6, 25.8 and 14.6 m/s. WP units are assumed to have identical generating turbines with a 2 MW rated capacity. In the base case, wind speed, load and bid uncertainties are assumed to be 3% (i.e. $\sigma/E = 3\%$). VCR is set to be $25,950/MWh [41]. The relative gap tolerance for the proposed Bender's decomposition algorithm is 10^{-4}. The model is solved by CPLEX using a PC with Intel Core i7-6600 CPU @ 2.80 GHZ with 8.00 GB RAM.

5.2 Garver's 6-bus system

As seen in Fig. 3, the original 6-bus system is composed of three thermal generators and one WP unit, seven branches (solid lines), and three loads. The peak load is 255 MW and total generation capacity is 480 MW. Three cases are used to demonstrate the effectiveness of the proposed approach.

Case 1: The proposed risk-averse TEP model.
Case 2: A risk-averse TEP model without DR.
Case 3: A deterministic security-constrained TEP model with DR.

The final planning scheme identified by the proposed approach for cases 1–3 is marked in Fig. 2 (dotted lines). The average daily load profiles for cases 1–3 are illustrated in Fig. 4. Compared with case 2, the load profiles for case 1 and 3 are more flat, since DR is used to provide ancillary services to balance WP and demand variations. Increment DR mainly occurs in the early morning, since WP fluctuations are bigger during that time in our studies. Decrement DR mainly occurs in peak hours (i.e. shaving peak demand), during which GC is relatively high. In addition, to protect the system against security issues, more DR is used in case 1 compared with case 3. Moreover, the detailed results of costs, including IC, GC, DRC, insecurity RC and total cost, are compared in Fig. 5. We can see that the deterministic security criterion in case three leads to conservative solutions and higher IC, GC and total cost are observed. This observation is also true when the WP penetration is increased to 100 MW in Fig. 6. Besides, higher WP penetration requires higher IC, meaning more lines are built to absorb the wind generation capacity. DRC also sees slight rises in cases 1 and 3, because more DR will be used to offset the fluctuations of WP, particularly when thermal units are constrained by their ramping limits. However, GC for all three cases decreases when WP capacity is increased from 50 MW in Fig. 5 to 100 MW in Fig. 6. Overall, the total costs for cases 1–3 all increase for higher WP penetration (increasing by 15, 24 and 20 M$ for cases 1–3, respectively).

Furthermore, we have given results of total costs, total WP curtailment (WPC), peak demand, total energy consumption, and EENS for different WP penetration levels in Tables 1 and 2. Note that EENS is calculated by minimising the total involuntary load curtailment under normal and contingency conditions (EENS $= \sum_{k=0}^{K} \sum_{t=1}^{8760} \sum_{i \in \Omega_D} P_{kit}^{\text{Curt}}$). The planning criterion in this paper is defined as that EENS should be less than 0.02% of total annual energy consumption. In Table 1, all cases satisfy the reliability criterion under $N-1$ conditions, while only case 1 can still meet it when $N-2$ conditions are considered (0.0187% < 0.02%). Moreover, in case 1, EENS is less than 0.02% under $N-1$ and $N-2$ conditions when WP capacity is 100 MW in Table 2 (0.0169% < 0.02% and 0.0198% < 0.02%). This demonstrates that the proposed approach can help to build a stronger network that can survive multiple contingencies with high WP penetration. Furthermore, from Tables 1 and 2, we can see that the changes in peak demands and total energy consumption are not evident for all three cases. The total WPC for case 2 is the largest (12986.89 MWh) since DR is not considered. This implies that DR plays an important role in helping WP integration.

5.3 IEEE 24-bus RTS system

The IEEE 24-bus RTS system is composed of 10 thermal stations, 38 branches and 20 loads. The peak load is 3404 MW and the total generation capacity of thermal units is 6000 MW. We assume that three WP farms are located at buses 2, 4, and 20, and they have an equal capacity at 200 MW (total WP capacity is 600 MW). The three cases in Section 5.2 are also used.

In addition, the advantages of using POPF, i.e. the point estimation method, are demonstrated by comparing it to the stochastic TEP, i.e. the MC simulation method. The convergence threshold of MC simulations is defined as the ratio of the standard deviation against the expected value is below 0.05. As seen in Fig. 7, the probability distributions of the total GC and DRC obtained by the two methods are quite similar. This means that the point estimation method can achieve an acceptable accuracy. Moreover, we have run the simulations using the two methods for 50 times, and the computational performance is compared by four indicators: the average (aver.), standard deviation (std.), minimum (min.), and maximum (max.) solution time. As seen in Table 3, the average simulation times for the point estimation and MC simulation methods are 1348 and 3594 s. Therefore, from the computational perspective, the point estimation method is much more efficient.

The identified planning schemes for cases 1–3 are given in Table 4. As seen, in order to alleviate network congestion, more lines are needed at parts where the meshed networks are weak. In generally, fewer lines are needed for case 1 and IC for case 1 is the lowest.

Fig. 8 illustrates the daily average WP output and curtailment. The deterministic approach in case 3 tends to use less WP compared with case 1, because the WP intermittency poses a

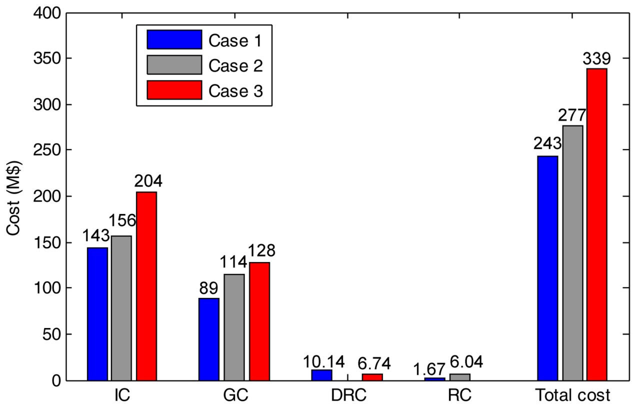

Fig. 5 *Results of costs for cases 1–3 with 50 MW WP capacity*

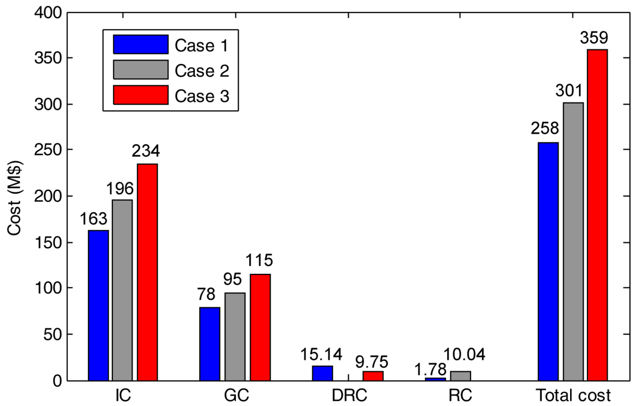

Fig. 6 *Results of costs for cases 1–3 with 100 MW WP capacity*

Table 1 Result comparison for cases 1–3 with 50 MW WP capacity

Case#	Total cost, M$	WPC, MWh	Peak demand, MW	Total energy, GWh	EENS	
					$N-1$, %	$N-2$, %
1	243.86	4235.68	293.12	970.21	0.0154	0.0187
2	276.78	9698.65	325.45	1000.05	0.0198	0.0365
3	338.84	5645.17	296.70	970.77	0.0186	0.0228

Table 2 Result comparison for cases 1–3 with 100 MW WP capacity

Case#	Total cost, M$	WPC, MWh	Peak demand, MW	Total energy, GWh	EENS	
					$N-1$, %	$N-2$, %
1	257.96	4322.36	293.12	980.27	0.0169	0.0198
2	300.78	12986.89	325.45	1010.09	0.0365	0.0594
3	358.84	6896.61	296.70	980.81	0.0278	0.0381

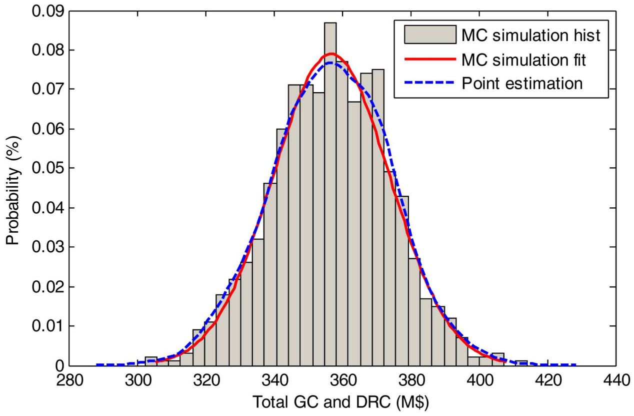

Fig. 7 *Probability distributions of total GC and demand response cost (DRC) on the 24-bus system*

Table 3 Computational performance by running 50 times of simulations on the IEEE 24-bus RTS system

Simulation time, s	Aver.	Std.	Min.	Max.
point estimation method	1348	16.21	1109	1784
MC simulation method	3594	36.97	3290	3899

Table 4 Planning schemes for cases 1–3

Case #	Identified planning schemes
1	$\eta_{1-3}=1,\ \eta_{2-6}=2,\ \eta_{11-13}=2,\ \eta_{15-16}=3,\ \eta_{15-21}=1,\ \eta_{20-23}=1$
2	$\eta_{1-3}=1,\ \eta_{1-5}=1,\ \eta_{3-9}=2,\ \eta_{6-10}=3,\ \eta_{11-13}=1,\ \eta_{12-23}=2$ $\eta_{15-16}=2, \eta_{17-22}=2, \eta_{19-20}=1, \eta_{20-23}=1$
3	$\eta_{1-3}=1, \eta_{1-5}=1, \eta_{4-9}=2, \eta_{8-9}=1, \eta_{11-14}=2, \eta_{12-23}=2,$ $\eta_{13-23}=1, \eta_{14-16}=3, \eta_{15-21}=1, \eta_{17-18}=2, \eta_{20-23}=1, \eta_{21-22}=2,$

significant insecurity risk on system operation and planning. Meanwhile, without DR, more WP is curtailed for case 2, since the thermal units are constrained by their ramping down limits when WP suddenly increases. Moreover, the detailed results of peak day GC and DR are shown in Fig. 9. Compared with case 3, more DR is used in case 1 to improve system security and help WP absorption. For case 1, the total increment DR is 1479 MWh and total decrement DR is 3873 MWh. For case 3, the total increment DR is 1108 MWh and the total decrement DR is 3248 MWh. More importantly, GC is the lowest for case 1, particularly the price spike at 19 pm for case 1 is the lowest. But this phenomenon is not obvious between cases 2 and 3.

In addition, Fig. 10 compares RC and EENS for cases 1 and 2 under different line contingencies. Note that the branches are numbered according to [39]. In most contingencies, RC and EENS for case 1 are lower. However, there are no trends of EENS or RC found across the studied contingencies. The highest RC for case 1 is $2032 for the outage of branch # 37, while for case 2 it is $3579 for the outage of branch # 31.

Furthermore, to validate the robustness of a planning scheme to the uncertainties of wind speed, load and DR bids, 64 validation scenarios are generated based on the mean and the standard deviation of the uncertainty parameters. Specifically, wind speed, load and DR bid uncertainties are generated by the combination of $\sigma/E = 1\%; 3\%; 5\%; 7\%$ (i.e. $4\times4\times4=64$ scenarios). A robustness evaluation index (REI) is defined according to the relative error of regrets [22]:

$$\text{Robustness} = \frac{1}{\hat{R}}\left|\hat{R} - \frac{1}{M}\cdot\sum_{i=1}^{M} R_i\right| \times 100\% \tag{44}$$

where R_i denotes the insecurity risk in scenario i, $\hat{R}$ denotes the risk of the obtained solution, M is the total number of scenarios; $1/M\cdot\sum_{i=1}^{M} R_i$ is the average insecurity risk in the validation scenarios. The practical meaning of REI indicates the closeness of

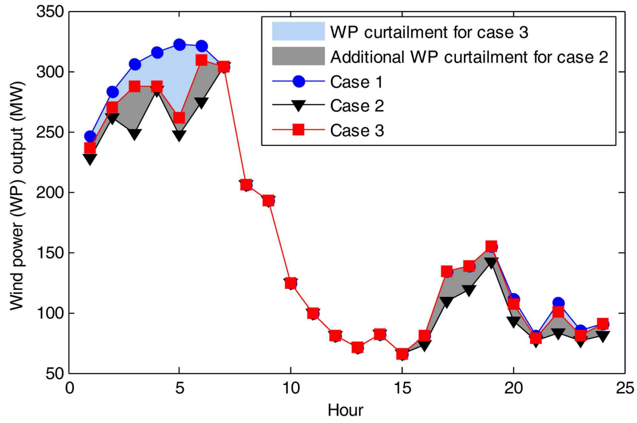

Fig. 8 *Daily average WP output and curtailment*

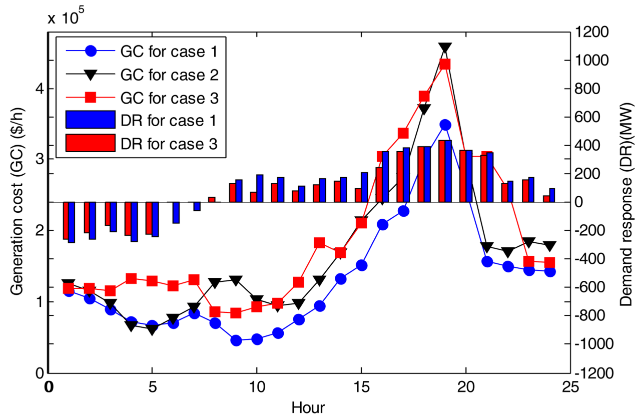

Fig. 9 *Peak day GC and DR*

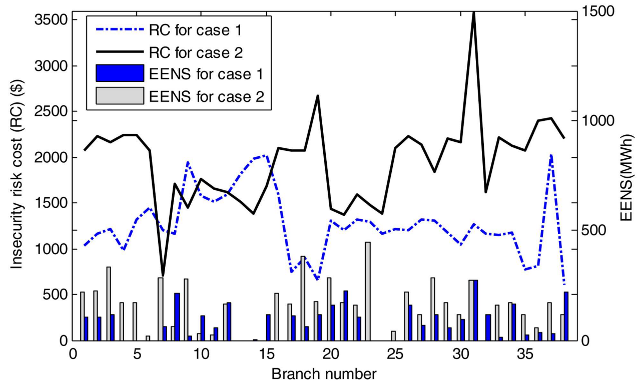

Fig. 10 *Insecurity RC and EENS for line contingencies*

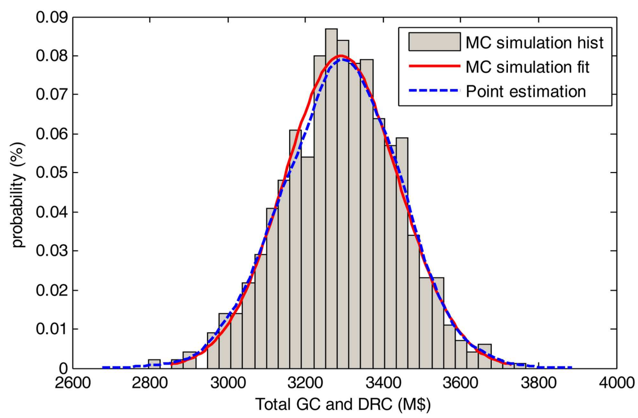

Fig. 11 *Probability distributions of total GC and DRC on the 2383-bus Polish system*

Table 5 Result comparison for cases 1–3 with 600 MW WP capacity

Case#	Total cost, M$	WPC, GWh	Peak demand, MW	Total energy, TWh	EENS		REI, %
					$N-1$, %	$N-2$, %	
1	494.53	22.23	3910	12.48	0.0165	0.0189	0.16
2	652.36	85.70	4344	12.84	0.0198	0.0253	0.86
3	815.65	52.15	3918	12.52	0.0186	0.0206	0.39

Table 6 Result comparison for cases 1–3 with 900 MW WP capacity

Case#	Total cost, M$	WPC, GWh	Peak demand, MW	Total energy, TWh	EENS		REI, %
					$N-1$, %	$N-2$, %	
1	501.38	28.65	3910	12.52	0.0185	0.0198	0.18
2	752.36	95.32	4344	12.93	0.0295	0.0458	0.98
3	998.71	56.32	3918	12.59	0.0216	0.0321	0.65

Table 7 Computational performance by running 50 times of simulations on the 2383-bus Polish system

Simulation time, s	Aver.	Std.	Min.	Max.
point estimation method	4467	89.71	4095	4790
MC simulation method	13,567	234.98	13,098	14,032

Table 8 Result comparison for cases 1–3 with 2500 MW WP capacity on the 2383-bus Polish system

Case#	Total cost, M$	WPC, GWh	Peak demand, MW	Total energy, TWh	EENS		REI, %
					$N-1$, %	$N-2$, %	
1	4516.54	183.96	28,298	89.45	0.0172	0.0196	0.27
2	6789.38	436.04	31,343	98.43	0.0199	0.0287	0.95
3	8034.12	324.56	29,094	89.97	0.0192	0.0258	0.46

the insecurity risk obtained to that under stochastic variations. A solution is said to be more robust, if the value of REI is smaller.

From Tables 5 and 6 we can see that REI for case 1 is the lowest with 600 and 900 MW WP capacities (0.16 and 0.18%, respectively). Besides, other results such as total cost, WPC, peak demand, and total energy consumption are also the lowest for case 1. By contrast, results of WPC, peak demand and total energy consumption are the highest for case 2 without the consideration of DR. Moreover, the deterministic approach in case 3 results in the highest total cost for the two WP penetration scenarios (815.65 and 998.71 M$). It is worth mentioning that with 600 MW WP, EENS satisfies the criterion for all cases under $N-1$. However, when WP increases to 900 MW or when $N-2$ conditions are considered, only case 1 can still satisfy the reliability criterion. The implications of these findings are: (i) if DR is optimally integrated into the objective function, DR can be efficiently used to balance WP outputs, reduce GC, defer capital investment, and improve system security and reliability. (ii) The proposed approach can better coordinate the dispatch of power generation and DR resources and mitigate WPC, thus improving the overall economic efficiency. (iii) Compared with the deterministic approach, the proposed risk-averse approach is more robust to stochastic variations and higher WP penetration.

5.4 2383-bus polish system

The peak load of the studied 2383-bus Polish system is 24,558 MW and the total generation capacity is 38,179 MW. We assume that five WP are located at buses 64, 730, 1024, 1875 and 2204, and they have an equal capacity at 500 MW (total WP capacity is 2500 MW). The three cases in Section 5.2 are also used. Furthermore, to validate the robustness of a planning scheme to the uncertainties of wind speed, load and DR bids, 125 validation scenarios are generated based on the mean and the standard deviation of the uncertainty parameters. Specifically, wind speed, load and DR bid uncertainties are generated by the combination of $\sigma/E = 1\%; 3\%; 5\%; 7\%; 9\%$ (i.e. $5 \times 5 \times 5 = 125$ scenarios).

Fig. 11 illustrates the probability distributions of total GC and DRC obtained by the point estimation and MC simulation methods. The computational performances of the two methods are compared in Table 7 by running 50 times of simulations. As seen in Fig. 11 and Table 7, compared with the MC simulation method, the point estimation method can provide a satisfactory estimation, while significantly reducing the computational burden (the average simulation time is reduced from 13,567 to 4467 s). Based on the results in Tables 3 and 7, we can conclude that the improvement in terms of the computational performance using the point estimation method is more evident on the bigger size network.

Furthermore, the results of total cost, WPC, peak demand, total energy, EENS and REI are compared for cases 1–3. The findings are similar to those in Section 5.3. As seen in Table 8, compared with the TEP model without DR (case 2) or the deterministic security-constrained TEP model in the existing works (case 3), the proposed approach (case 1) is superior. Specifically, the proposed model requires the lowest cost, reduces the WP curtailment, peak demand and total energy consumption, and improves the system reliability. Also, the proposed approach is more robust to uncertainties (the REI for case 1 is the lowest at 0.27%).

6 Conclusion

WP and DR programs play an important role in ensuring energy sustainability and improving system efficiency. On the other hand, the large-scale integration of WP and DR introduces increasing uncertainties to TEP. This paper has proposed a risk-averse TEP framework to address the insecurity risk in relation to future uncertainties. The conventional deterministic security criterion is replaced by a risk measure, which can capture the probabilistic nature of system behaviours such as WP outputs, load variations, DR bids and component availability. The formulated TEP objective is comprised of line IC, power GC, DRC, insecurity RC. To enhance the computational efficiency, an iterative algorithm based on the Benders decomposition in conjunction with POPF is employed and developed to solve the formulated TEP model. The proposed risk-averse TEP approach is verified on the Garver's 6-bus, IEEE 24-bus RTS and 2383-bus Polish systems and comparative studies have been undertaken. According to the simulation results, the impacts of WP and DR on system security and adequacy can be effectively investigated. The proposed approach can better coordinate the dispatch of power generation and DR resources and mitigate WPC, thus improving the overall economic efficiency. More importantly, the proposed risk-averse approach is more robust to stochastic variations and higher WP penetration. Therefore, network planners can use the proposed approach to hedge against the future investment risks in relation to uncertainties.

7 Acknowledgment

The work in this paper is supported by a China Southern Power Grid Research Grant WYKJ00000027, the National Natural Science Foundation of China (Key Program 71331001, 71420107027, 91547113 and General Program 71071025, 71271033), the Science and Technology Projects of Hunan Province and Changsha City (2016WK2015, kh1601186) and the Shenzhen Municipal Science and Technology Innovation Committee International R&D project (GJHZ20160301165723718).

8 References

[1] Khodaei, A., Shahidehpour, M., Wu, L., *et al.*: 'Coordination of short-term operation constraints in multi-area expansion planning', *IEEE Trans. Power Syst.*., 2012, **27**, (4), pp. 2242–2250

[2] Maghouli, P., Hosseini, S.H., Buygi, M.O., *et al.*: 'A scenario-based multi-objective model for multi-stage transmission expansion planning', *IEEE Trans. Power Syst.*, 2011, **26**, (1), pp. 470–478

[3] Qiu, J., Dong, Z.Y., Zhao, J., *et al.*: 'A risk-based approach to multi-stage probabilistic transmission network planning', *IEEE Trans. Power Syst.*, 2016, **31**, (6), pp. 4867–4876

[4] Li, C.X., Dong, Z.Y., Chen, G., *et al.*: 'Flexible transmission expansion planning associated with large-scale wind farms integration considering demand response', *IET. Gener. Transm. Distrib.*, 2015, **9**, (15), pp. 2276–2283

[5] Ozdemir, O., Munoz, F.D., Ho, J.L., *et al.*: 'Economic analysis of transmission expansion planning with price-responsive demand and quadratic losses by successive LP', *IEEE Trans. Power Syst.*, 2016, **31**, (2), pp. 1096–1107

[6] de J Silva, I., Rider, M.J., Romero, R., *et al.*: 'Transmission network expansion planning with security constraints', *IET. Gener. Transm. Distrib.*, 2005, **152**, (6), pp. 828–836

[7] Van Cutsem, T., Vournas, C.: '*Voltage stability of electric power systems*' (Kluwer, Norwell, MA, 1998)

[8] Billinton, R., Allan, R.: '*Reliability evaluation of power systems*' (Plenum Press, New York, 1996, 2nd edn.)

[9] Billinton, R., Yi, G., Karki, R.: 'Application of a joint deterministic-probabilistic criterion to wind integrated bulk power system Planning', *IEEE Trans. Power Syst.*, 2010, **25**, (3), pp. 1384–1392

[10] Roh, J.H., Shahidehpour, M., Wu, L.: 'Market-based generation and transmission planning with uncertainties', *IEEE Trans. Power Syst.*, 2009, **24**, (3), pp. 1587–1598

[11] Alizadeh, B., Dehghan, S., Amjady, N., *et al.*: 'Robust transmission system expansion considering planning uncertainties', *IET. Gener. Transm. Distrib.*, 2013, **7**, (11), pp. 1318–1331

[12] Park, H., Baldick, R.: 'Transmission planning under uncertainties of wind and load: sequential approximation approach', *IEEE Trans. Power Syst.*, 2013, **28**, (3), pp. 2395–2402

[13] Gu, Y., McCalley, J.D., Ming, N.: 'Coordinating large-scale wind integration and transmission planning', *IEEE Trans. Sustain. Energy*, 2012, **3**, (4), pp. 652–659

[14] Munoz, C., Sauma, E., Contreras, J., *et al.*: 'Impact of high wind power penetration on transmission network expansion planning', *IET. Gener. Transm. Distrib.*, 2012, **6**, (12), pp. 1281–1291

[15] Alguacil, N., Motto, A.L., Conejo, A.J.: 'Transmission expansion planning: A mixed-integer LP approach', *IEEE Trans. Power Syst.*, 2003, **18**, (3), pp. 1070–1077

[16] Alhamrouni, I., Khairuddin, A., Ferdavani, A.K., *et al.*: 'Transmission expansion planning using AC-based differential evolution algorithm', *IET. Gener. Transm. Distrib.*, 2014, **8**, (10), pp. 1637–1644

[17] Choi, J., Tran, T., El-Keib, A.A., *et al.*: 'A method for tranmission system expansion planning considering probabilistic reliability criteria', *IEEE Trans. Power Syst.*, 2005, **29**, (3), pp. 1606–1615

[18] Kazerooni, A.K., Mutale, J.: 'Transmission network planning under security and environmental constraints', *IEEE Trans. Power Syst.*, 2010, **25**, (2), pp. 1169–1178

[19] Zhang, H., Vittal, V., Heydt, G.T., *et al.*: 'A mixed-integer linear programming approach for multi-stage security-constrained transmission expansion planning', *IEEE Trans. Power Syst.*., 2012, **27**, (2), pp. 1125–1133

[20] Ugranli, F., Karatepe, E.: 'Transmission expansion planning for wind turbine integrated power systems considering contingency', *IEEE Trans. Power Syst.*, 2016, **31**, (2), pp. 1476–1485

[21] Rahmani, M., Romero, R., Rider, M.J.: 'Risk/investment-driven transmission expansion planning with multiple scenarios', *IET. Gener. Transm. Distrib.*, 2013, **7**, (2), pp. 154–165

[22] Alvarez Lopez, J., Ponnambalam, K., Quintana, V.H.: 'Generation and transmission expansion under risk using stochastic programming', *IEEE Trans. Power Syst.*, 2007, **22**, (3), pp. 1369–1378

[23] Zhao, J.H., Dong, Z.Y., Lindsay, P., *et al.*: 'Flexible transmission expansion planning with uncertainties in an electricity Market', *IEEE Trans. Power Syst.*, 2009, **24**, (1), pp. 479–488

[24] Arroyo, J., Manuel, N.A., Carrion, M.: 'A risk-based approach for transmission network expansion planning under deliberate outages', *IEEE Trans. Power Syst.*, 2010, **25**, (3), pp. 1759–1766

[25] Shrestha, G.B., Fonseka, P.A.J.: 'Congestion-driven transmission expansion in competitive power markets', *IEEE Trans. Power Syst.*, 2004, **19**, (3), pp. 1658–1665

[26] Conejo, A.J., Carrion, M., Morales, J.M.: '*Decision making under uncertainty in electricity markets*' (Springer, New York, NY, USA, 2010)

[27] Nguyen, D.T., Negnevitsky, M., Groot, M.d.: 'Market-based demand response scheduling in a degregulated environment', *IEEE Trans. Smart Grid*, 2013, **4**, (4), pp. 1948–1956

[28] Mashhour, E., Moghaddas-Tafreshi, S.M.: 'Bidding strategy of virtual power plant for participating in energy and spinning reserve markets-part I: problem formulation', *IEEE Trans. Power Syst.*, 2011, **26**, (2), pp. 949–956

[29] Abdollahi, A., Moghaddam, M.P., Rashidinejad, M., *et al.*: 'Investigation of economic and environmental-driven demand response measures incorporating UC', *IEEE Trans. Smart Grid*, 2012, **3**, (1), pp. 12–25

[30] Zhao, J.H., Wen, F.S., Dong, Z.Y., *et al.*: 'Optimal dispatch of electric vehicles and wind power using enhanced particle swarm optimization', *IEEE Trans. Ind. Inf.*, 2012, **8**, (4), pp. 889–899

[31] Beltran, B., Ahmed-Ali, T., Benbouzid, M.E.H.: 'High-order sliding-mode control of variable-speed wind turbines', *IEEE Trans. Ind. Electron.*, 2009, **56**, (9), pp. 3314–3321

[32] Hong, H.P.: 'An efficient point estimate method for probabilistic analysis', *Reliab. Eng. Syst. Saf.*, 1998, **59**, (3), pp. 261–267

[33] Eydeland, A., Wolyniec, K.: '*Energy and power risk management*' (Wiley, Chichester, UK, 2003)

[34] Xu, Y., Dong, Z.Y., Zhang, R., *et al.*: 'Solving preventive-corrective SCOPF by a hybrid computational strategy', *IEEE Trans. Power Syst.*, 2014, **29**, (3), pp. 1345–1355

[35] Asadamongkol, S., Eua-arporn, B.: 'Transmission expansion planning with AC model based on generalized Benders decomposition', *Int. J. Electr. Power Energy Syst.*, 2013, **47**, pp. 402–407

[36] Munoz, F.D., Hobbs, B.F., Watson, J.P.: 'New bounding and decomposition approaches for MILP investment problems: Multi-area transmission and generation planning under policy constraints', *Eur. J. Oper. Res.*, 2016, **248**, (3), pp. 888–898

[37] Majidi-Qadikolai, M., Baldick, R.: 'Stochastic transmission capacity expansion planning with special scenario selection for integrating $N-1$ contingency analysis', *IEEE Trans. Power Syst.*, 2016, **31**, (6), pp. 4901–4912

[38] Wu, H., Shahidehpour, M., Al-Abdulwahab, A.: 'Hourly demand response in day-ahead scheduling for managing the variability of renewable energy', *IET. Gener. Transm. Distrib.*, 2013, **7**, (3), pp. 226–234

[39] Reliability Test System Task Force of Probability Methods Sub-committee: 'IEEE reliability test system', *IEEE Trans.*, 1979, **PAS-98**, pp. 2047–2054

[40] Matpower 5.0-Description of case 2383wp. Available at http://www.pserc.cornell.edu/matpower/docs/ref/matpower5.0/case2383wp.html

[41] Australian Energy Market Operator (AEMO)-Value of Customer Reliability (VCR) review. Available at http://www.aemo.com.au/Electricity/National-Electricity-Market-NEM/Planning-and-forecasting/Value-of-Customer-Reliability-review